

Short Communication

## Metal-insulator-semiconductor-insulator-metal structure of TiO<sub>2</sub>/SiO<sub>2</sub> Thin Films for Ultraviolet (UV) Photodetectors

Tung-Te Chu<sup>1</sup>, Yu-Jen Hsiao<sup>2</sup>, Liang-Wen Ji<sup>3,\*</sup>, and Jhih-Wei Yang<sup>3</sup>

<sup>1</sup>Department of Mechanical Engineering and Automation Engineering, Kao Yuan University, No. 1821, Jhongshan Rd., Lujhu Township, Kaohsiung County, 821 Taiwan, R.O.C.

<sup>2</sup>National Nano Device Laboratories, National Applied Research Laboratories, Tainan 741, Taiwan

<sup>3</sup>The Institute of Electro-Optical and Materials Science, National Formosa University. No. 64, Wenhua Rd., Huwei, Yunlin 632, Taiwan, R.O.C.

\*E-mail: [lwji@nfu.edu.tw](mailto:lwji@nfu.edu.tw), [lwji@seed.net.tw](mailto:lwji@seed.net.tw)

Received: 22 April 2015 / Accepted: 12 August 2015 / Published: 30 September 2015

---

In this report, the silver electrodes of metal-insulator-semiconductor-insulator-metal (MISIM) structure ultraviolet (UV) photodetectors (PDs) based on TiO<sub>2</sub> thin films were fabricated. The device was grown on corning glass by radio frequency magnetron sputtering (RF-sputtering) technique. The results exhibit significant improvement in the performance of photocatalytic properties and conductivities under a function of annealing conditions. It can be found that dark current of different structure photodetectors were  $1.28 \times 10^{-10}$  (MSM-PDs) 、  $1.76 \times 10^{-11}$  (MISIM-PDs) at 5V bias. Demonstrably, it presents that the dark current should be reduced in MISIM structure. Meanwhile, the value of responsivity would become bigger during the annealing temperature increasing, respectively.

---

**Keywords:** TiO<sub>2</sub>, photodetectors, metal-insulator-semiconductor-insulator- metal structured.

### 1. INTRODUCTION

Recently, many researchers have explored the ultraviolet (UV) photodetectors for their commercial and military applications, such as space communication, flame detection, biology, environmental monitoring, and so on [1-5]. With the advent of optoelectronic devices fabricated on wide band gape. TiO<sub>2</sub>, ZnO, and GaN became promising materials in making UV photodetectors [6-9]. In TiO<sub>2</sub>, many researchers are interested in the photoelectric properties recently. Titanium dioxide (TiO<sub>2</sub>) is a wide band-gap semiconductor material that is sensitive in UV region as well as applications

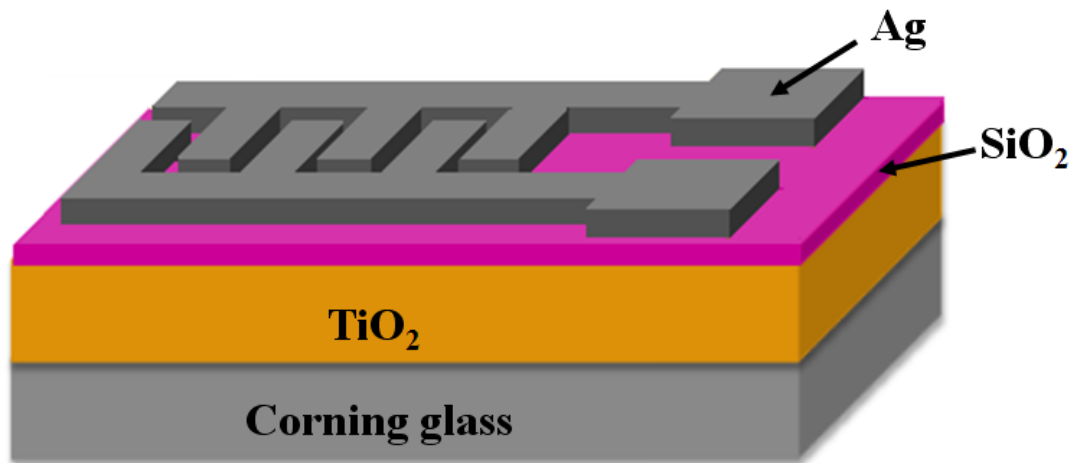
for biological, oxygen sensitivity, catalysis, and solar energy conversion. The anatase TiO<sub>2</sub> structure has interested a lot of attention within the last decades for its technological applications such as photovoltaic solar cells and photodetectors (PDs) with promising efficiency. They have researched in many areas, such as solar cell, temperature sensor, and etc. [10-13]. With TiO<sub>2</sub>-based, the UV photodiodes are also used in commercial photodevices. The hybrid UV photodetectors based on a TiO<sub>2</sub> nanorod array and polyfluorene was showed by Han et al. It is a good photoconductive effect and can be seen that the TiO<sub>2</sub> nanostructures improved the photoresponsivity in devices [14]. The metal-semiconductor-metal (MSM) structure UV PDs have been investigated in recent years [15-18]. The metal–semiconductor–metal (MSM) TiO<sub>2</sub> UV detectors with a high photoresponsivity of about 889.6 A/W were presented by Kong et al. It was higher than those of other wide band gap UV detectors with a MSM structure [19]. Nevertheless, the responsivity of these PDs could be not reached our prospect because the photo-generated carriers were trapped by the structural imperfections on the surface of the films. It is to insert an insulating layer (SiO<sub>2</sub>) between the metal contacts could be the way for solving the problem.

In this study, the metal-insulator-semiconductor-insulator-metal (MISIM) structure was fabricated based on TiO<sub>2</sub> thin films. As comparing with MSM structure UV PDS under same conditions, the results show significant improvement in the performance of photocatalytic properties and conductivities. Meanwhile, the optical and electrical performance of the metal-insulator-semiconductor-insulator-metal (MISIM) structure was also explored in the paper.

## 2. EXPERIMENTAL

During deposition, a TiO<sub>2</sub> and SiO<sub>2</sub> target with 3-in diameter and purity of 99.99 % were used. The TiO<sub>2</sub>/SiO<sub>2</sub> thin films were deposited on corning glass substrates by radio frequency magnetron sputtering (RF-sputtering) technique under different thickness (TiO<sub>2</sub>, 300nm; SiO<sub>2</sub>, 20nm and 40nm). During growth, the working pressure of the chamber was about 5×10<sup>-2</sup> torr, the RF power was 100 W, and the gas mixing ratio Ar/O<sub>2</sub>=10/1, and then the TiO<sub>2</sub> seed layer was annealed for 2 hours. The films were annealed under different temperature 300°C, 400°C, and 500°C and be investigated by XRD and UV-VIS.

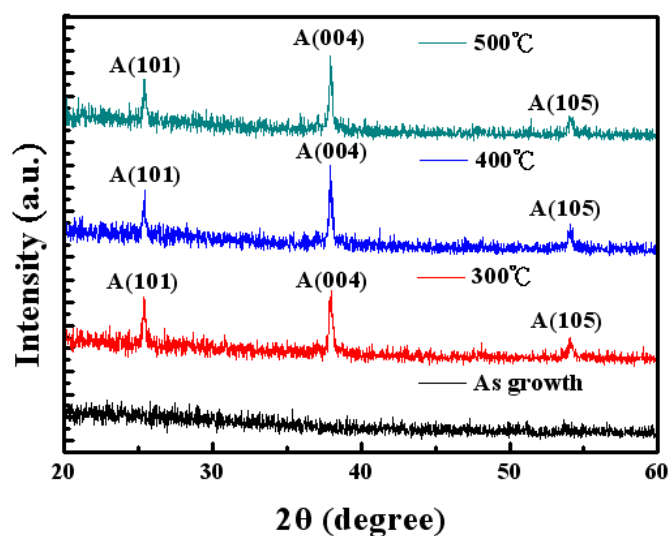
The silver electrodes of metal-insulator-semiconductor-insulator-metal (MISIM) structure ultraviolet (UV) photodetectors (PDs) based on TiO<sub>2</sub> thin films were then fabricated. Prior to the deposition of contact electrodes, wafers were dipped in acetone and methanol to clean the surface. A 100nm thick Ag film was subsequently deposited onto the sample surface by e-gun evaporation to serve as the metal contact. The fingers of the Ag contact electrodes were 10µm wide and 150µm long, with 10µm spacing. The active area of the whole device was 150 × 160µm<sup>2</sup>. Fig. 1 is the MISIM structure TiO<sub>2</sub> UV photodetectors. The photocurrent, dark current, and responsivity of photodetectors were then measured by a HP4156C semiconductor parameter analyzer. The spectral response of MSM UV PDs was measured by a light source which employed a 300 W Xe lamp and a monochromator covering the range of 250~600 nm.



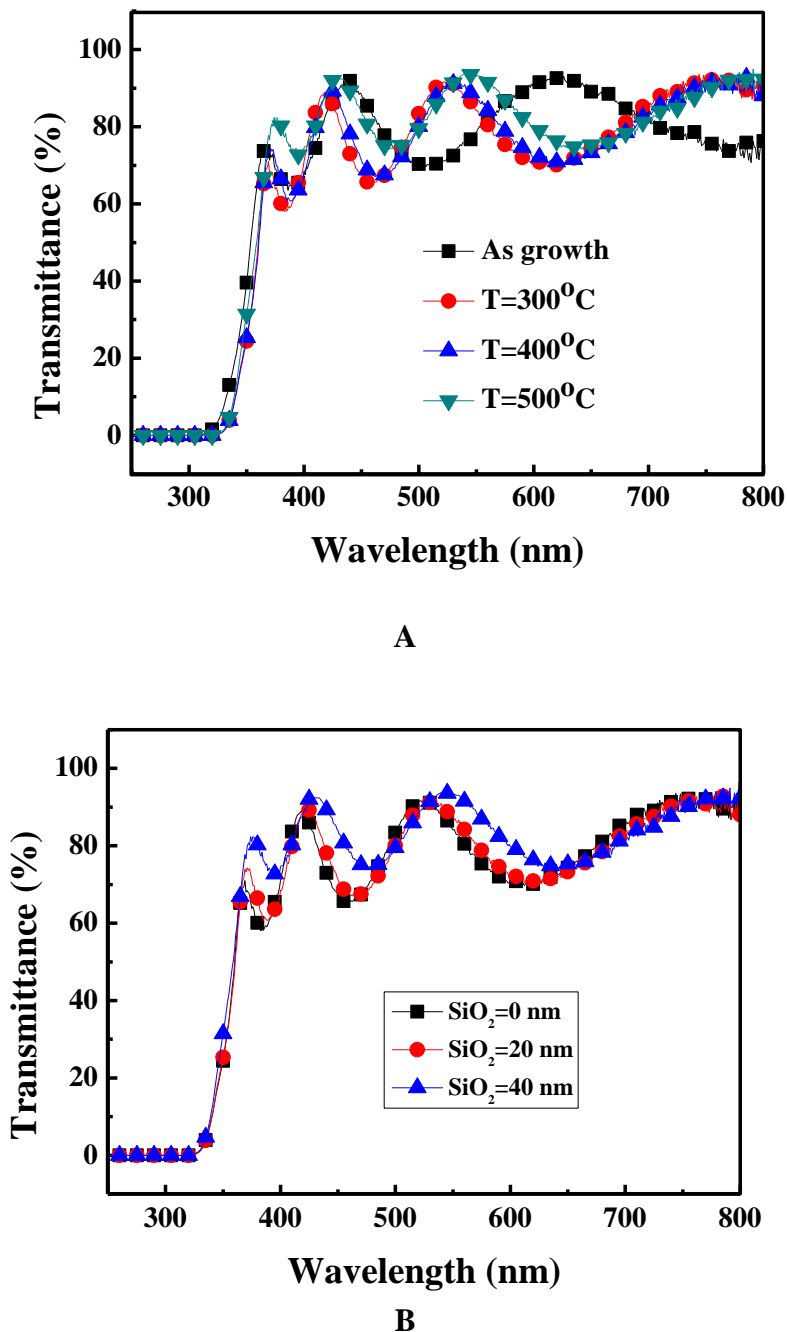
**Figure 1.** The caption of the MISIM structured TiO<sub>2</sub> UV PDs.

### 3. RESULTS AND DISCUSSION

The TiO<sub>2</sub> semiconductor by sputter exhibits the characteristic peaks of anatase structure in X-Ray diffraction (XRD) analysis, as shown in Fig. 1. XRD spectra also indicate the TiO<sub>2</sub> film presents a strong (004) preferred orientation at  $2\theta=37.78$  corresponding to anatase phases. The other prominent peaks corresponded to the (101) and (105) directions. The full width at half maximum (FWHM) of the diffraction peak is rather small, which indicates that the film crystallinity is fairly good. It show measured XRD spectrum of the TiO<sub>2</sub> thin films under different annealing temperature. The results showed that the TiO<sub>2</sub> was anatase structure above 300 °C annealing. Three diffraction peaks occurred at (101), (004), and (105) planes, respectively. It was found that the annealing temperature was higher, the diffraction peaks were stronger.



**Figure 2.** The XRD (X-ray diffraction) patterns of TiO<sub>2</sub> thin films 300nm with different temperature.



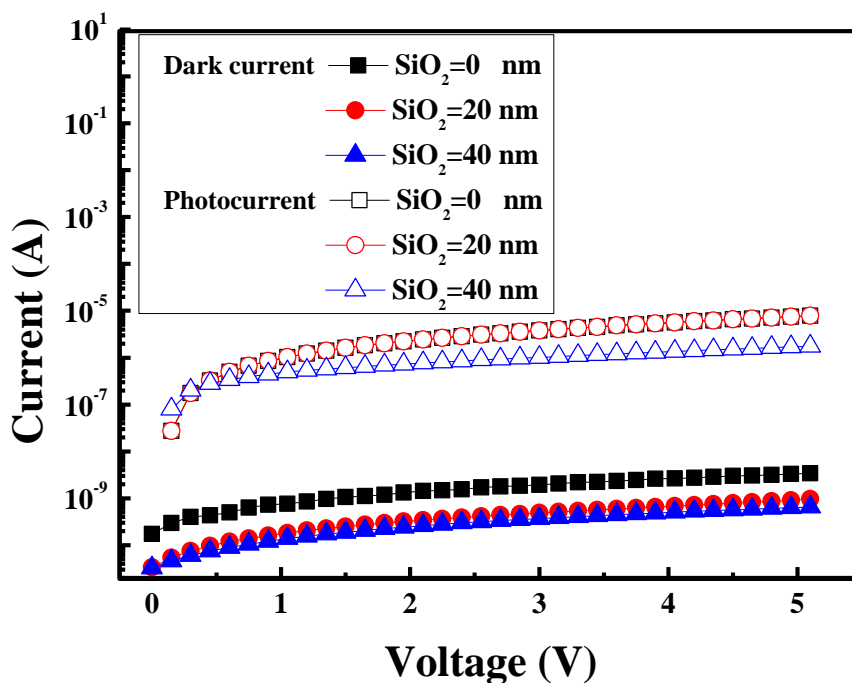
**Figure 3.** (a) Transmission spectrum of TiO<sub>2</sub> thin films (300nm) under different temperature (b) Transmission spectrum of TiO<sub>2</sub> thin films (300nm) under different SiO<sub>2</sub> thicknesses in 300°C annealing temperature.

Fig. 3a shows the optical transmittance obtained from the TiO<sub>2</sub> thin films are under various temperatures heat treatment. The transparency of the film increased more than 2% between near UV and visible after annealing from 81.3% to 83.8% as temperature increased to 500 °C. It suggests that the crystallization could be increased by thermal diffusion. In addition, the transmittance peak of the film towards a longer wavelength after annealing. This can be attributed to the TiO<sub>2</sub> crystal phase transfer during the heat treatment. In Fig. 3b, it show the UV-Vis transmission spectra of TiO<sub>2</sub> thin

films are under various SiO<sub>2</sub> thicknesses. It showed that the SiO<sub>2</sub> thickness increased, the transmittance increased too. The transparency of the film increased about 2.5% after deposition SiO<sub>2</sub> film from 80.8% to 83.3% as thickness increased to 40 nm.

The probability reason can explain this phenomena for SiO<sub>2</sub> film following with high transmittance: (i) the lower effective refractive index and (ii) the graded-index profile due to the texture antireflection layer [20].

As shown in Fig.4, the I-V characteristics on TiO<sub>2</sub> photodetectors are in different SiO<sub>2</sub> thicknesses under 5V bias and 340nm illumination. The data indicates that the dark current of MISIM PDs is smaller than MSM PDs. Obviously, it presents that the dark current should be reduced in MISIM structure. With 5 V applied bias, the photocurrent to dark current contrast ratios of the TiO<sub>2</sub> and SiO<sub>2</sub>/TiO<sub>2</sub> PDs were 1300 and 2400, respectively. Photocurrent of the TiO<sub>2</sub> film and SiO<sub>2</sub>/TiO<sub>2</sub> PDs based at 5 V were  $1.39 \times 10^{-7}$  and  $7.23 \times 10^{-8}$  A, respectively. The dark current and photocurrent of TiO<sub>2</sub> thin films (300nm) under different temperature and different SiO<sub>2</sub> thicknesses in 340nm illumination at 5V bias were shown at table 1. The SiO<sub>2</sub>/TiO<sub>2</sub> were more suitable to increase optical absorption that is because the SiO<sub>2</sub>/TiO<sub>2</sub> film having antireflection effect than TiO<sub>2</sub> film. However, the dark current of the SiO<sub>2</sub>/TiO<sub>2</sub> film is very small. This may be due to the low background carrier concentration. It is well known that oxygen vacancies exist in n-type semiconducting titania acting as donors, besides the SiO<sub>2</sub>/TiO<sub>2</sub> film have few insulation layer that can provide lower carrier concentration and less active sites [21].



**Figure 4.** The current-voltage (I-V) characteristics for the fabricated TiO<sub>2</sub> (300nm) UV PDs under different SiO<sub>2</sub> thicknesses in 500°C annealing temperature.

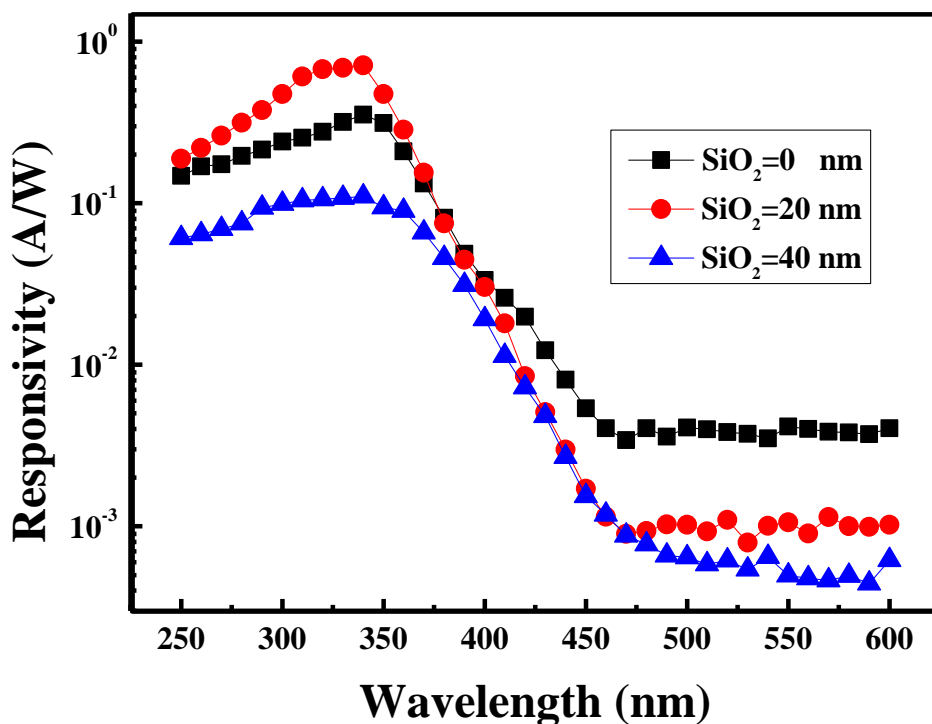


**Figure 5.** The relation of the responsivity and wavelength in TiO<sub>2</sub> (300nm) UV PDs under different SiO<sub>2</sub> thicknesses in 500°C annealing temperature

**Table 1.** The dark current and photocurrent of TiO<sub>2</sub> thin films (300nm) under different temperature and different SiO<sub>2</sub> thicknesses in 340nm illumination at 5V bias

Sample	Dark current (A)	Photocurrent(A)
SiO <sub>2</sub> 0nm T=300°C	$1.07 \times 10^{-10}$	$1.39 \times 10^{-7}$
SiO <sub>2</sub> 20nm T=300°C	$4.52 \times 10^{-11}$	$7.19 \times 10^{-7}$
SiO <sub>2</sub> 40nm T=300°C	$3.03 \times 10^{-11}$	$7.23 \times 10^{-8}$
SiO <sub>2</sub> 0nm T=400°C	$9.82 \times 10^{-10}$	$9.11 \times 10^{-7}$
SiO <sub>2</sub> 20nm T=400°C	$2.39 \times 10^{-10}$	$2.29 \times 10^{-6}$
SiO <sub>2</sub> 40nm T=400°C	$1.60 \times 10^{-10}$	$3.20 \times 10^{-7}$
SiO <sub>2</sub> 0nm T=500°C	$3.42 \times 10^{-9}$	$7.82 \times 10^{-6}$
SiO <sub>2</sub> 20nm T=500°C	$9.6 \times 10^{-10}$	$7.82 \times 10^{-6}$
SiO <sub>2</sub> 40nm T=500°C	$6.49 \times 10^{-10}$	$1.76 \times 10^{-6}$

Figure 5 presented the responsivity and UV-to-visible rejection ration on TiO<sub>2</sub> PDs in different annealing temperature and SiO<sub>2</sub> thicknesses at 10V bias. In the 300nm TiO<sub>2</sub> thin film, under the different thermal annealing temperature (300°C, 400°C, and 500°C), the reponsivity is  $6.54 \times 10^{-4}$  A/W,  $7.01 \times 10^{-3}$  A/W, and  $3.54 \times 10^{-1}$  A/W and the UV-to-visible rejection ration is individuated in 63, 80, and 98.7. Therefore, the results show that the responsivity of the MISIM PHDs is significantly improved.

The responsivity and UV-to-visible rejection ratio of TiO<sub>2</sub> thin films (300nm) under different temperature and different SiO<sub>2</sub> thicknesses at 5V bias were shown at table 2.

The responsivity of a detector (R) is defined as

$$R = \frac{I_p}{P_{inc}} = \eta \frac{\lambda(\mu m)}{1.24} A/W \quad (1)$$

**Table 2.** The responsivity and UV-to-visible rejection ratio of TiO<sub>2</sub> thin films (300nm) under different temperature and different SiO<sub>2</sub> thicknesses at 5V bias

Sample	Light source	Responsivity (A/W)	UV-to-visible rejection ratio	
SiO <sub>2</sub> 0nm T=300°C	340 nm	6.54×10 <sup>-4</sup>	340 nm/490 nm	63
SiO <sub>2</sub> 20nm T=300°C	340 nm	1.1×10 <sup>-3</sup>	340 nm/490 nm	357
SiO <sub>2</sub> 40nm T=300°C	340 nm	2.69×10 <sup>-4</sup>	340 nm/490 nm	142
SiO <sub>2</sub> 0nm T=400°C	340 nm	7.01×10 <sup>-3</sup>	340 nm/490 nm	80
SiO <sub>2</sub> 20nm T=400°C	340 nm	7.13×10 <sup>-3</sup>	340 nm/490 nm	463
SiO <sub>2</sub> 40nm T=400°C	340 nm	1.44×10 <sup>-3</sup>	340 nm/490 nm	147
SiO <sub>2</sub> 0nm T=500°C	340 nm	3.54×10 <sup>-1</sup>	340 nm/490 nm	98.7
SiO <sub>2</sub> 20nm T=500°C	340 nm	7.16×10 <sup>-1</sup>	340 nm/490 nm	695
SiO <sub>2</sub> 40nm T=500°C	340 nm	1.10×10 <sup>-1</sup>	340 nm/490 nm	167

where  $I_p$ ,  $P_{inc}$ ,  $\eta$ , and  $\lambda$  are the photocurrent, the quantum efficiency and the incident light wavelength, respectively. Assume all the photons are absorbed by semiconductor ( $\eta = 1$ ) and 340 nm to the expression. Comparing the SiO<sub>2</sub>/TiO<sub>2</sub> structure with the traditional TiO<sub>2</sub> film, it can be observed that some ions diffuse at the titanium dioxide layers after annealing. The diffusion process reduces the defect structure and series resistance reflectivity. Besides, the maximum responsivity shifted to higher wavelength after adding SiO<sub>2</sub> layer due to the top material reflection effect. In addition, the spectral presented a passband response between 340 nm and 490 nm. With such a definition, it was found that UV-to-visible rejection ratios with 20 nm SiO<sub>2</sub> film of the PDs were 463 and 695 for 400 °C and 500 °C, respectively. It should be note that internal gain exists in the fabricated devices. The devices exhibit a high photoresponsivity of 0.716 A/W, which corresponds to an internal gain is 100. These oxygen vacancies of TiO<sub>2</sub> film act as recombination centers and capturing the photo-induced holes [22]. Under an operating voltage, the photo-induced electrons would be collected easily by the passive layer such as SiO<sub>2</sub> film. Therefore, the photogenerated holes are difficult to recombine with the electrons, which enhance the carrier lifetime and the internal gain[23-24]. In this study, the novelty of TiO<sub>2</sub>/SiO<sub>2</sub> thin films with appropriate thickness and annealing provided formation of photocurrent and dark current pathways and improved the responsivity of ultraviolet (UV) photodetectors (PDs).

#### 4. CONCLUSION

As demonstrated above, the MISIM PDs are explored and compared with MSM PDs. The data indicated that the dark current of different structure photodetectors were 1.28×10<sup>-10</sup> (MSM-PDs) 、

$1.76 \times 10^{-11}$  (MISIM-PDs) at 5V bias. Demonstrably, it presents that the dark current should be reduced in MISIM structure. It also presented that the annealing temperature or the thickness of SiO<sub>2</sub> thin film increased, it would influence the transmittance, respectively. Meanwhile, the data also indicated that the responsivity of the MISIM PHDs outperforms the MSM PHDs. As a conclusion, the results clearly reveal that the former (MISIM) exhibits significant improvement in the performance of photocatalytic properties and conductivities over the latter (MSM).

## Reference

1. M. Liao, Y. Koide, *Appl. Phys. Lett.* 89 (2006) 113509.
2. M. Razeghi, A. Rogalski, *J. Appl. Phys.* 79 (1996) 7433.
3. Monroy E, Omnes F, Calle F. *Semicond Sci Technol* 2003;18(4):R33e51.
4. Goldberg YA. *Semicond Sci Technol* 1999;14(7):R41e60.
5. Averine SV, Kuznetsov PI, Zhitov VA, Alkeev NV. *Solid-State Electron* 2008;52 (5):618e24.
6. H.M. Kim, T.W. Kang, K.S. Chung, *Adv. Mater.* 15 (2003) 567.
7. H. He Jr., S.T. Ho, T.B. Wu, L.J. Chen, Z.L. Wang, *Chem. Phys. Lett.* 435 (2007) 119.
8. X.G. Zheng, Q.Sh. Li, J.P. Zhao, D. Chen, B. Zhao, Y.J. Yang, L.Ch. Zhang, *Appl. Surf. Sci.* 253 (2006) 2264.
9. H.L. Xue, X.Z. Kong, Z.R. Liu, *Appl. Phys. Lett.* 90 (2007) 201118.
10. D. Kwon, K.M. Kim, J.H. Jang, J.M. Jeon, M.H. Lee, G.H. Kim, X. Li, G. Park, B. Lee, S.Han, M. Kim, C.S. Hwang, *Nat. Nanotechnol.* 5 (2010) 148.
11. K. Zhu, N.R. Neale, A. Miedaner, A.J. Frank, *Nano Lett.* 7 (2007) 69.
12. Z. Li, H. Zhang, W. Zheng, W. Wang, H. Huang, C. Wang, A.G. MacDiarmid, Y. Wei, *J. Am. Chem. Soc.* 130 (2008) 5036.
13. U. Kirner, K.D. Schierbaum, W. Göpel, B. Leibold, N. Nicoloso, W. Weppner, D. Fischer, W.F. Chu, *Sens. Actuators, B* 1 (1990) 103.
14. Y. Han, G. Wu, M. Wang, H. Chen, *Appl. Surf. Sci.* 256 (2009) 1530.
15. S. Liang, H. Sheng, Y. Liu, Z. Huo, Y. Lu, H. Shen, *J. Cryst. Growth* 225 (2001) 110.
16. Q.A. Xu, J.W. Zhang, K.R. Ju, X.D. Yang, X. Hou, *J. Cryst. Growth* 289 (2006) 44.
17. W. Yang, R.D. Vispute, S. Choopun, R.P. Sharma, T. Venkatesan, H. Shen, *Appl. Phys. Lett.* 78 (2001) 2787.
18. D.Y. Jiang, J.Y. Zhang, K.W. Liu, Y.M. Zhao, C.X. Cong, Y.M. Lu, B. Yao, Z.Z. Zhang, D.Z. Shen, *Semicond. Sci. Technol.* 22 (2007) 687.
19. X. Kong, C. Liu, W. Dong, X. Zhang, C. Tao, L. Shen, J. Zhou, Y. Fei, S. Ruan, *Appl. Phys. Lett.* 94 (2009) 123502.
20. Y. Liang, Z. Xu, J. Xia, S. T. Tsai, Y. Wu, G. Li, C. Ray, L. Yu, *Adv. Mater.* 22, (2010) E135.
21. L. W. Ji, Y.J. Hsiao, S.J. Young, W.S. Shih, W. Water, and S.M. Lin, *IEEE Sensors Journal*, 15 (2015) 762.
22. O. Sheikhejad-Bishe, F. Zhao, A. Rajabtabar-Darvishi, E. Khodadad, A. Mostofizadeh1 and Y. Huang, *Int. J. Electrochem. Sci.*, 9 (2014) 4230.
23. J.L. Hou, S.J. Chang, S.P. Chang, *Int. J. Electrochem. Sci.*, 8 (2013) 5650.
24. S.P. Chang, *Int. J. Electrochem. Sci.*, 8 (2013) 10280.